Infrared Spectrum of the Fundamental Vibration–Rotation Band of $^3\Sigma^-$ OH$^+$

Mark W. Crofton, Robert S. Altman,† Mary-Frances Jagod, and Takeshi Oka*

Department of Chemistry and Department of Astronomy and Astrophysics, The University of Chicago, Chicago, Illinois 60637 (Received: June 27, 1985)

The fundamental $v = 1 \leftarrow 0$ vibration–rotation band of the $^3\Sigma^-$ OH$^+$ ion has been observed by using the tunable infrared radiation from a difference frequency system and the velocity modulation technique of detection. The band origin was determined to be $\nu_0 = 2956.3724$ (29) cm^{-1}. The rotational constant B, the centrifugal distortion constant D, and the spin–spin and the spin–rotation constants λ and γ have been determined for the ground and for the first excited states. It was found that the discharge condition for the effective production of OH$^+$ (and H$_2$O$^+$) is very different from that for H$_3$O$^+$. The ion–molecule reactions leading to the formation of OH$^+$ in the discharge are discussed.

Introduction

Infrared spectroscopy of molecular ions using frequency tunable laser radiation sources and discharges has recently been applied to many fundamental molecular ions.[1] Most of the molecular ions studied by this method are protonated ions HX$^+$ in which a proton is attached to stable molecules and atoms to form closed-shell structures. Because of the high proton affinities of stable molecules and atoms, the protonated ions are often the end products in the chain of molecular reactions in the discharge of H$_2$:X mixtures.

In this paper we report our application of the same method to the open-shell OH$^+$ molecular ion which belongs to a different category of ions. The discharge conditions to produce this type of ion abundantly are considerably different from those commonly used for protonated ions. In the discharge described later in detail, the usually strong H$_3$O$^+$ lines are barely visible, but the lines of OH$^+$ and H$_2$O$^+$ are clearly observable. We summarize our results on OH$^+$ in this paper; the spectrum of H$_2$O$^+$ will be published later in a separate paper.

The vibration–rotation constants of OH$^+$ have already been well determined from the detailed study of the optical emission spectrum by Merer and his colleagues.[2] The history and earlier spectroscopic papers on this molecular ion are summarized in the paper. The ground electronic state has the symmetry $^3\Sigma^-$, and therefore a triplet structure is expected. This ion has been detected in comets through the optical spectrum by Fehrenbach and Ar-

pigny.[3] Very recently Saykally and colleagues have observed rotational transitions of this molecule in the far infrared region by laser magnetic resonance.[4] During preparation of this paper we also learned that Dymanus and colleagues have observed the $J = 1 \leftarrow 0$ rotational transition in the submillimeter wave region.[5]

Experiment

A difference frequency laser system developed by Pine[6] was used as the frequency tunable infrared source. A small-bore (4 mm i.d.) water-cooled ac discharge cell with the length of 1 m was used as the absorption cell. A gas mixture of 100:1:1 He:O$_2$:H$_2$ at the total pressure of 10 torr gave the best results. Because of the small diameter of the discharge tube, a minimum pressure of ~4 torr was needed to maintain a stable ac discharge. The He:H$_2$O mixture used by Merer et al.[2] also gave absorption signals in a water-cooled cell and in a liquid-N$_2$-cooled cell; however, both He:H$_2$O and He:H$_2$:O$_2$ mixtures gave weaker signals at liquid N$_2$ temperature. The powerful velocity modulation technique introduced by Gudeman, Saykally, and others[7]

(1) C. S. Gudeman and R. J. Saykally, *Annu. Rev. Phys. Chem.*, **35**, 387 (1984).
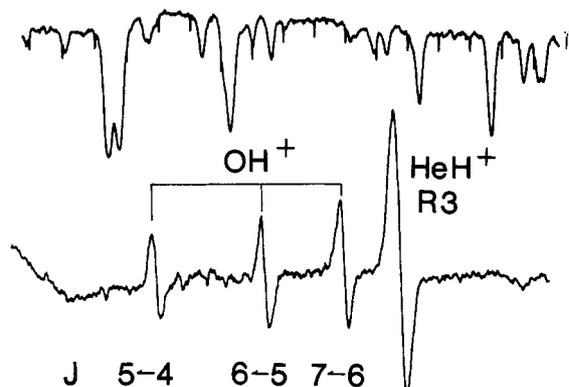(2) A. J. Merer, D. N. Malm, R. W. Martin, M. Horani, and J. Rostas, *Can. J. Phys.*, **53**, 251 (1975).
(3) C. Fehrenbach and C. Arpigny, *C. R. Acad. Sci. Paris, Ser. B* **277**, 569 (1973).
(4) R. J. Saykally, private communication.
(5) J. P. Bekooy, P. Verhoeve, W. L. Meerts, and A. Dymanus, *J. Chem. Phys.*, in press.
(6) A. S. Pine, *J. Opt. Soc. Am.*, **64**, 1783 (1974).

†Present address: Perkin Elmer Corporation, 2000 York Road, Oak Brook, IL 60521.

Figure 1. The triplet lines of the R(5) transitions of OH^+ which appear very close to the R(3) line of HeH^+. A small-bore (4 mm i.d.) water-cooled ac discharge cell with a $He:O_2:H_2$ gas mixture of $\sim100:1:1$ was used with the total pressure of ~10 torr. The total number densities of OH^+ and HeH^+ are estimated to be $9 \times 10^9/cm^3$ and $2 \times 10^9/cm^3$, respectively.
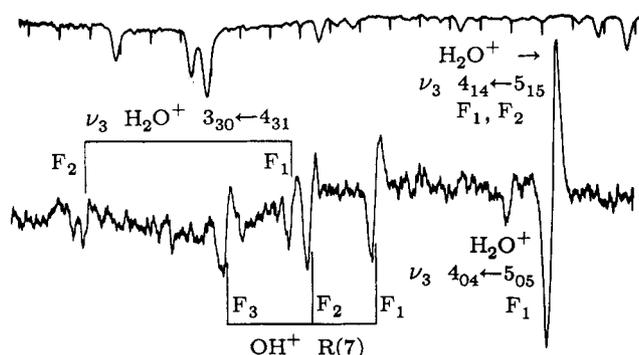
Figure 2. The triplet lines of the R(7) transition of OH^+ which appear close to the $3_{30} \leftarrow 4_{31}$ and $4_{14} \leftarrow 5_{15}$ transitions of the ν_3 band of H_2O^+.

was used to discriminate ion lines from much stronger neutral lines and to increase the detection sensitivity. The ac discharge was maintained at the p–p voltage of ~7 kV and the rms current of ~65 mA. Because of the small bore of the discharge cell, unidirectional multiple passing was not possible. We have also used a larger bore (12 mm i.d.) discharge cell with six unidirectional traversals at pressures from 4 to 10 torr, which led to a comparable signal-to-noise ratio. It seems that the small bore discharge cell produces an ion concentration which is several times more than the larger discharge cell, presumably because of the higher current density (~500 vs. ~50 mA/cm^2). Noise subtraction[8] was used to reduce the laser source noise. The infrared spectral lines of C_2H_4 accurately measured by Pine[9] were used as the frequency standard.

Observed Spectrum

Typical examples of observed lines of OH^+ are shown in Figures 1 and 2. Figure 1 shows the triplet lines corresponding to the R(5) transitions of OH^+ which happen to be very close to the R(3) line of the HeH^+ ion that is also seen very strongly in the trace. This trace was recorded with the small-diameter (4 mm i.d.) discharge cell and the high-pressure (10 torr) mixture of $He:H_2:O_2$ (100:1:1). The width of the HeH^+ line is larger than that of the OH^+ lines by a factor of 2 because of larger random velocities. From the observed absolute intensities for the OH^+ lines and the HeH^+ line ($\Delta I/I = 5 \times 10^{-5}$ and 1.5×10^{-4}, respectively), the theoretical dipole moments (0.175^{10} and 0.364^{11-13}), and the ro-

(7) C. S. Gudeman, M. H. Begemann, J. Pfaff, and R. J. Saykally, *Phys. Rev. Lett.*, **50**, 727 (1983).

(8) D. J. Nesbitt, H. Petek, C. S. Gudeman, C. B. Moore, and R. J. Saykally, *J. Chem. Phys.* **81**, 5281 (1984).

(9) A. S. Pine, M.I.T. Lincoln Laboratory Report No. NSF/ASRA/DAR-78-24562, 1980.

(10) H. J. Werner, P. Rosmus, and E. A. Reinsch, *J. Chem. Phys.*, **79**, 905 (1983).

TABLE I: Observed Frequencies of the $X^3\Sigma^-$ OH^+ $v = 1 \leftarrow 0$ Fundamental Band

		ν_{obsd}, cm^{-1}	$\Delta\nu^a$				ν_{obsd}, cm^{-1}	$\Delta\nu^a$
R(7)	$F_3 \leftarrow F_3$	3163.212	-1	P(1)	$F_1 \leftarrow F_1$		2923.943	3
	$F_2 \leftarrow F_2$	3163.069	-1		$F_1 \leftarrow F_2$		2921.895	-1
	$F_1 \leftarrow F_1$	3163.964	3	P(2)	$F_1 \leftarrow F_1$		2889.541	-2
R(6)	$F_3 \leftarrow F_3$	3143.203	-3		$F_2 \leftarrow F_2$		2889.261	1
	$F_2 \leftarrow F_2$	3143.050	0		$F_3 \leftarrow F_3$		2887.655	0
	$F_1 \leftarrow F_1$	3142.934	1		$F_2 \leftarrow F_3$		2891.778	-2
R(5)	$F_3 \leftarrow F_3$	3121.463	-1	P(3)	$F_1 \leftarrow F_1$		2853.887	0
	$F_2 \leftarrow F_2$	3121.291	0		$F_2 \leftarrow F_2$		2853.650	-1
	$F_1 \leftarrow F_1$	3121.164	0		$F_3 \leftarrow F_3$		2853.236	0
R(4)	$F_3 \leftarrow F_3$	3098.032	1	P(4)	$F_1 \leftarrow F_1$		2816.945	0
	$F_2 \leftarrow F_2$	3097.828	-1		$F_2 \leftarrow F_2$		2816.727	0
	$F_1 \leftarrow F_1$	3097.689	-1		$F_3 \leftarrow F_3$		2816.462	1
R(3)	$F_3 \leftarrow F_3$	3072.962	1	P(5)	$F_1 \leftarrow F_1$		2778.749	-2
	$F_2 \leftarrow F_2$	3072.704	1		$F_2 \leftarrow F_2$		2778.540	0
	$F_1 \leftarrow F_1$	3072.546	1		$F_3 \leftarrow F_3$		2778.323	3
R(2)	$F_3 \leftarrow F_3$	3046.370	1	P(6)	$F_1 \leftarrow F_1$		2739.248	-3
	$F_2 \leftarrow F_2$	3045.950	0		$F_2 \leftarrow F_2$		2739.143	1
	$F_1 \leftarrow F_1$	3045.762	-2		$F_3 \leftarrow F_3$		2738.940	0
R(1)	$F_2 \leftarrow F_2$	3017.612	1					
	$F_1 \leftarrow F_1$	3017.367	-2					
R(0)	$F_2 \leftarrow F_1$	2989.353	2					
	$F_1 \leftarrow F_1$	2987.324	-1					

$^a \Delta\nu = (\nu_{obsd} - \nu_{calcd}) \times 10^3$ (in cm^{-1}).

tational temperature of ~500 K determined approximately from the relative intensities of different rotational lines, the concentrations of the two ions are calculated to be $9 \times 10^9/cm^3$ and $2 \times 10^9/cm^3$, respectively. The larger diameter (12 mm i.d.) discharge cell produced several times less OH^+ but the observed signal was comparable because of the unidirectional multiple passing. Figure 2 shows the R(7) transitions of OH^+ which happen to be close to the $4_{14} \leftarrow 5_{15}$ and the $3_{30} \leftarrow 4_{31}$ transitions of the H_2O^+ ion. We cannot estimate the H_2O^+ concentration accurately because the theoretical transition dipole moment is not available, but the H_2O^+ concentration seems to be comparable to the OH^+ concentration.

The observed frequencies are shown in Table I together with the residues of the least-squares fitting. We used the Miller–Townes formulae for the rotational levels of $^3\Sigma$ molecules[14]

$$F_1(J=N+1) = B_vN(N+1) + B_v(2N+3) - \lambda - \frac{\gamma}{2} - $$
$$\left[\lambda^2 - 2\lambda\left(B_v - \frac{\lambda}{2}\right) + (2N+3)^2\left(B_v - \frac{\gamma}{2}\right)^2\right]^{1/2}$$

$$F_2(J=N) = B_vN(N+1)$$

$$F_3(J=N-1) = B_vN(N+1) - B_v(2N-1) - \lambda - \frac{\gamma}{2} - $$
$$\left[\lambda^2 - 2\lambda\left(B_v - \frac{\gamma}{2}\right) + (2N-1)^2\left(B_v - \frac{\gamma}{2}\right)^2\right]^{1/2}$$

where the rotational constant B_v is replaced by the effective value $B_{eff} = B_v - D_vN(N+1)$, N is the rotational quantum number, and λ and γ are the spin–spin and the spin–rotation interaction constants, respectively. The simpler Schlapp formulae[15] gave identical results except for the band origin because of the different combination of ν_0 and λ and γ in the two formalisms. More detailed formulae by Amano and Hirota[16] and the inclusion of

(11) S. Peyerimhoff, *J. Chem. Phys.*, **43**, 998 (1965).

(12) H. H. Michels, *J. Chem. Phys.*, **44**, 3834 (1966).

(13) I. Dabrowski, and G. Herzberg, *Trans. N.Y. Acad. Sci.*, Ser II, **38**, 1 (1977).

(14) S. L. Miller and C. H. Townes, *Phys. Rev.*, **90**, 537 (1953).

(15) R. Schlapp, *Phys. Rev.*, **51**, 342 (1937).

TABLE II: Vibration–Rotation Constants for the $X^3\Sigma^-$ OH$^+$ $v = 1 \leftarrow$ 0 Fundamental Band^a

	this work	ref 2^b	ref 5^c
B_0	16.42294 (31)	16.42233 (77)	16.422889 (9)
D_0	0.00191894 (609)	0.00191744 (242)	
λ_0	2.1457 (30)	2.1344 (115)	2.142983 (18)
γ_0	-0.1496 (10)	-0.1478 (14)	-0.151195 (12)
B_1	15.69494 (24)	15.69490 (92)	
D_1	0.0018607 (35)	0.0018694 (67)	
λ_1	2.1353 (28)	2.1361 (80)	
γ_1	-0.1448 (9)	-0.1442 (12)	
ν_0	2959.3724 (29)	2956.34 (4)	

^{a}All values are in cm^{-1}. Parenthetical values are uncertainties (3σ) in the units of the last significant figure quoted. ^{b}Merer et al. ^{c}Bekooy et al.

TABLE III: Derived Molecular Constants of $X^3\Sigma^-$ OH$^+$ in cm^{-1}

$\alpha^B - 2\gamma^B$	0.72800 (39)	r_e	1.02893 (1) Å
α^λ	0.0104 (41)	B_e	16.7952 (10)^a
α^γ	-0.0048 (13)	λ_e	2.1510 (36)
		γ_e	-0.1520 (13)

^{a}In determining B_e, the value of $\gamma^B = 0.01097$ cm^{-1} by Merer et al. (ref 2) was assumed.

the rotational dependences of λ and γ as well as the sextic centrifugal distortion constant H were found unnecessary for the present accuracy of measurement ($\sim$0.003 cm^{-1}). The observed transitions are of $\Delta J = \Delta N$ type except for the R(0), P(1), and P(2) transitions where $F_1 \leftrightarrow F_2$ and $F_2 \leftrightarrow F_3$ transitions are also observed. A nonlinear least-squares fitting routine by parabolic extrapolation[17] was used.

The determined constants are listed in Table II together with the earlier results of Merer et al.[2] The accuracy of vibration and rotation constants is improved significantly except for the values of the centrifugal distortion constants. Also listed in Table II are the recent submillimeter results of Bekooy et al.[5] which are in good agreement with our results for the ground-state constants. The constants B_v, λ_v, and γ_v determined for $v = 1$ and $v = 0$ have been used to derive equilibrium molecular constants and the vibrational dependence of these constants. The derived molecular constants are listed in Table III. The vibrational dependence of λ and γ were derived from the difference of λ_1 and λ_0, and γ_1 and γ_0, respectively. The difference of B_1 and B_0 contains a significant contribution from the nonlinear term γ^B which has been determined to be 0.01097 cm^{-1} by Merer et al.[2] The equilibrium rotational constant B_e and the equilibrium internuclear distance r_e have been derived by assuming this value of γ^B.

Formation of OH$^+$ in the Discharge

Usually the H$_3$O$^+$ ion is the dominating ionic species in a gaseous discharge containing H$_2$ and O$_2$. We have seen, however, that if H$_2$ and O$_2$ are diluted with much He, we can suppress the strong H$_3$O$^+$ signals and produce OH$^+$ and H$_2$O$^+$ abundantly. The OH$^+$ and H$_2$O$^+$ ions were not observed in discharges containing only H$_2$ and O$_2$. We have also seen that a mixture of He and a small fraction of H$_2$O produces slightly reduced OH$^+$ and H$_2$O$^+$ signals. OH$^+$ was also observed in a discharge of Ar:H$_2$:O$_2$ $\simeq$ 100:1:1. The pumping speed did not seem to affect the OH$^+$ concentration critically.

Several channels can be considered for the formation of OH$^+$ in the He:O$_2$:H$_2$ discharge. However, our calculation of reaction rates shows that the most efficient channel starts from the production of O$^+$ by the ionization dissociation of O$_2$ due to metastable He atoms and plasma electrons. This process is slower[18] than the production of O$_2^+$ or H$_2^+$ but the resultant O$^+$ produces OH$^+$ very

efficiently through the ion–molecule reaction

$$O^+ + H_2 \rightarrow OH^+ + H \tag{1}$$
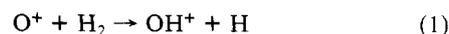
which is exothermic (0.6 eV) and has a Langevin rate.[19]

The reactions of O$_2^+$($^2\Pi_g$) with H$_2$ are endothermic and require high translational energy for their efficient execution.[20] It is known[21,22] that much O$_2^+$ is produced in the metastable $^4\Pi$ state upon ionization of O$_2$. For such O$_2^+$ ions, the reactions with H$_2$ are exothermic and produce HO$_2^+$ efficiently. However, the reactions leading to OH$^+$ and H$_2$O$^+$ have been shown to be inefficient by Lindinger et al.[23] The reactions of H$_2^+$ (or H$_3^+$ which is produced abundantly from H$_2^+$) with O$_2$ are exothermic and produce O$_2^+$ and HO$_2^+$ efficiently but they do not appear to break the O$_2$ bond to produce OH$^+$ and H$_2$O$^+$.[24] The reaction of H$_2^+$ and H$_3^+$ with the O atom to produce OH$^+$ has the Langevin cross section but is not efficient because of the small abundance of O in the discharge. In the He–H$_2$O mixture OH$^+$ is produced directly by the dissociative ionization of H$_2$O.

The OH$^+$ ion is destroyed either by H$_2$ through the ion–molecule reaction

$$OH^+ \xrightarrow[-H]{H_2} H_2O^+ \xrightarrow[-H]{H_2} H_3O^+ \tag{2}$$
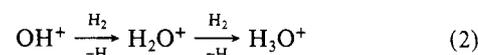
or by O$_2$ through the charge exchange reaction[19]

$$OH^+ + O_2 \rightarrow O_2^+ + OH \tag{3}$$
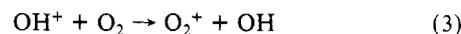
The former reaction which has a Langevin rate constant (1.5 × 10^{-9} cm^3/s) leads to the H$_3$O$^+$ ion. The latter reaction interrupts the sequence of eq 2 and reduces the H$_3$O$^+$ concentration with the increased O$_2^+$ concentration. The rate constant for the charge exchange reaction is smaller ($k \sim 2 \times 10^{-10}$ cm^3/s) for the ground-state O$_2$ but is probably much larger for O$_2$ in the metastable state which exists abundantly in the discharge. The interruption of the sequence is also effected by the ion exchange between H$_2$O$^+$ and O$_2$ which occurs with a similar rate constant. Thus it has earlier been observed[25] in the H$_2$–O$_2$ discharge that the increased O$_2$ concentration reduces the amount of H$_3$O$^+$ drastically. The end ion products of eq 2 and 3, H$_3$O$^+$ and O$_2^+$, are stable and destroyed by electronic recombination and the ambipolar diffusion to the wall.

The role of He for increasing the relative concentration of OH$^+$ and H$_2$O$^+$ must be (a) to increase the rate of O$^+$ production by metastable He atom and by increased electron temperature (which is proportional to the ionization potential[26]) in the discharge and more importantly (b) to reduce the rates of the reactions 2 and 3 by dilution so that their rates are not many orders of magnitude larger than the destruction rates of H$_3$O$^+$ and O$_2^+$ by electron recombination and ambipolar diffusion. For the high-pressure (10 torr) discharge in the small-bore (4 mm i.d.) tube, the electron density in the plasma is estimated by N_e (I/S)/eV to be $\sim$1.5 × 10^{12} cm^{-3}, for the current density $I/S = 500$ mA/cm^2 and the electron drift velocity $v = 2 \times 10^6$ cm/s (a discharge electric field of $\sim$24 V/cm was assumed.[26] The electron temperature in the plasma is estimated to be $\sim$35 000 K from the Figures 124 and 130 of ref 26. Thus using the electron recombination rate constant given by McGowan et al.[27] and the relation $k \sim E_e^{1/2}$, we obtain

(16) T. Amano and E. Hirota, *J. Mol. Spectrosc.*, **53**, 346 (1974).
(17) P. Bevington, "Data Reduction and Error Analysis for the Physical Sciences", McGraw-Hill, New York, 1969.
(18) L. J. Kieffer, *At. Data*, **1**, 19 (1969).

(19) F. C. Fehsenfeld, A. L. Schmeltekopf, and E. E. Ferguson, *J. Chem. Phys.*, **46**, 2802 (1967).
(20) M. M. Chiang, E. A. Gislason, B. H. Mahan, C. W. Tsao, and A. S. Werner, *J. Phys. Chem.*, **75**, 1426 (1971).
(21) M. Tadjeddine, R. Aboual, P. C. Crosby, B. A. Huber, and J. T. Moseley, *J. Chem. Phys.*, **69**, 710 (1978).
(22) A. Carrington, P. G. Roberts, and P. J. Sarre, *Mol. Phys.*, **35**, 512 (1978).
(23) W. Lindinger, D. L. Albritton, M. McFarland, F. C. Fehsenfeld, A. L. Schmeltekopf, and E. E. Ferguson, *J. Chem. Phys.*, **62**, 4101 (1975).
(24) J. K. Kim and W. J. Huntress, Jr., *J. Chem. Phys.*, **62**, 2820 (1975).
(25) D. J. Liu, N. N. Haese, and T. Oka, *J. Chem. Phys.*, in press.
(26) A. von Engel, "Ionized Gases", Oxford University Press, London, 1955.
(27) J. W. McGowan, P. M. Mul, V. S. D'Angelo, J. B. A. Mitchell, P. Defrance, and H. R. Forelich, *Phys. Rev. Lett.*, **42**, 373 (1979).

the electron recombination rate of 2×10^4 and 5×10^4 s^{-1} for H_3O^+ and O_2^+, respectively. The ambipolar diffusion rate is on the order of 10^4 s^{-1} from the reduced mobility of 21 cm^2/(V s).[28] These destruction rates are smaller than the rates for eq 2 and 3 by a factor ~ 100.

Although we have no means to measure the concentration of O_2^+ in the discharge, the above analysis suggests that it is on the order of 10^{12}/cm^3. The concentrations of H_3O^+, OH^+, and H_2O^+ are $\sim 10^{10}$/cm^3.

(28) R. Johnsen, H. L. Brown, and M. A. Biondi, *J. Chem. Phys.*, **52**, 5080 (1970).